# SWITCHING THRESHOLD AND CODING-RATE OPTIMISATION FOR TURBO CONVOLUTIONAL AND TURBO BCH CODED ADAPTIVE MODULATION

*T. H. Liew and L. Hanzo*

Dept. of ECS., Univ. of Southampton, SO17 1BJ, UK.
Tel: +44-703-593 125, Fax: +44-703-593 045
Email: thl,lh@ecs.soton.ac.uk, http://www-mobile.ecs.soton.ac.uk

## ABSTRACT

**Decision Feedback Equaliser (DFE) aided turbo coded wideband Adaptive Quadrature Amplitude Modulation (AQAM) is capable of accommodating the temporal channel quality variation of fading channels. A procedure is suggested for determining the AQAM switching thresholds and the specific turbo coding rates capable of maintaining the target BER, while aiming for achieving a high effective Bits Per Symbol (BPS) throughput. Subsequently, the performances of both turbo convolutional (TC) and turbo BCH (TBCH) coded fixed and adaptive modulation schemes are characterised and compared when communicating over the COST 207 Typical Urban (TU) wideband fading channel. It was found that at a given throughput the set of TBCH coded fixed modulation schemes considered outperforms the corresponding TC counterparts, when using a high-latency turbo and channel interleaver. However, both schemes have a similar performance, when applied in conjunction with adaptive modulation.**

## 1. INTRODUCTION

Adaptive Quadrature Amplitude Modulation (AQAM) [1, 2] employs a higher-order modulation scheme, when the channel quality is favourable, in order to increase the number of Bits Per Symbol (BPS) transmitted and conversely, a more robust lower-order modulation scheme is activated, when the channel exhibits a reduced instantaneous quality, for the sake of improving the mean Bit Error Ratio (BER) performance. When applying AQAM for transmission over wideband channels, the decision feedback equaliser (DFE) employed will eliminate most of the Inter Symbol Interference (ISI). Consequently, the associated pseudo-Signal to Noise Ratio (SNR) at the output of the DFE, which will be defined in the context of Equation 1, is calculated and used as a metric for activating the appropriate modulation modes. This ensures that the performance is optimised by employing channel equalised AQAM, in order to jointly combat the signal power variations as well as the Co-Channel Interference (CCI) and ISI fluctuations experienced in a wideband channel. Recently the error correction and detection capability of various channel coding schemes [3] was exploited for improving the achievable BER and BPS throughput performance of wideband AQAM [4–6].

In order to achieve best possible BPS performance of a given target BER, the AQAM mode swicthing thresholds have to be optimised. In our earlier research we used a set of fixed AQAM mode switching thresholds, which was determined with the aid of Powell's or experimental optimisation [1,2,7]. However, the achievable throughput of the system can be further increased, when we optimise the AQAM switching thresholds for each individual channel SNR value using Lagrangian optimisation [1,8]. We note however that the solutions outlined in [1, 8] use no channel coding during the Lagrangian optimisation of the AQAM thresholds. Since employing Lagrangian optimisation might not be feasible for AQAM systems using turbo codes, we propose in this contribution a simple procedure for determining the AQAM switching thresholds and the highest-throughput coding rates for turbo coded AQAM systems, which aims for maximising the throughput at each average channel SNR value. In this context, the performance of turbo convolutional (TC) and turbo BCH (TBCH) codes [3] is compared in conjunction with both fixed and adaptive modulation.

VTC 2003 Spring, Jeju, Korea

## 2. SYSTEM OVERVIEW

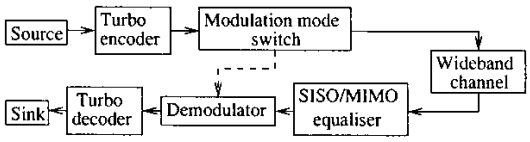


Figure 1: System overview of the turbo coded AQAM and space-time trellis schemes.

Figure 1 shows the system overview of the proposed turbo coded AQAM scheme. At the transmitter, the information source generates random information data bits. In our proposed turbo coded AQAM scheme, the information data bits are encoded by the turbo encoder. Assuming that the next transmission burst's short term channel quality can be estimated as in a Time Division Duplexing (TDD) scheme, a suitable AQAM mode will be chosen by the modulation mode switch shown in the figure. The turbo coded bits are subsequently mapped to the AQAM symbols. The modulated symbols are transmitted over the COST 207 TU wideband channel. At the receiver, the received symbols are equalised by the DFE. Depending on the specific AQAM mode chosen at the transmitter, the demodulator provides soft outputs for the turbo decoder based on the equalised symbols output by the equaliser. The turbo decoded bits are passed to the information sink for the calculation of the BER, as shown in Figure 1.

At the receiver, the channel impulse response (CIR) is estimated, which is then used for calculating the DFE coefficients [1, 2]. Subsequently, the DFE is used for equalising the ISI-corrupted received signal. Additionally, both the channel quality estimate and the DFE coefficients are utilised for computing the pseudo-SNR at the output of the DFE. By assuming that the residual ISI is Gaussian distributed and that the probability of decision feedback

0-7803-7757-5/03/$17.00 ©2003 IEEE.

errors is negligible, the pseudo-SNR at the output of the DFE, $\gamma$, can be calculated as [9]:

$$\gamma = \frac{\text{Wanted Signal Power}}{\text{Residual ISI Power + Effective Noise Power}}. \quad (1)$$

The pseudo-SNR, $\gamma$ is then compared against a set of AQAM switching threshold levels and subsequently the appropriate modulation mode is selected for the next transmission burst, assuming the availability of a reliable, low-delay feedback message, which can be transmitted to the remote receiver by superimposing it - after strongly protecting it - on the reverse-direction information [2]. However, in this treatise we will dispense with explicit AQAM mode signalling. The AQAM modes that are utilised in this system are Binary Phase Shift Keying (BPSK), Quadrature Phase Shift Keying (QPSK), 16-level Quadrature Amplitude Modulation (16QAM), 64-level Quadrature Amplitude Modulation (64QAM) and a 'No Transmission' (NO TX) mode.

## 3. SIMULATION PARAMETERS

As we can see in Figure 1, turbo codes [3] are concatenated with the AQAM scheme. Both convolutional and block codes can be used as component codes in a turbo code. It was shown by Hagenauer *et al.* [10] that turbo block codes outperform punctured turbo convolutional codes, when the coding rate is higher than $R = \frac{2}{3}$. In this contribution we will investigate the performance of turbo BCH (TBCH) and turbo convolutional (TC) codes, when using various fixed modulation schemes and AQAM. Table 1 shows the parameters of each turbo codec used in the system.

| Code | Octal generator polynomial | No. of states | Decoding algorithm | No. of iterations |
|---|---|---|---|---|
| **Turbo Convolutional Code (TC)** | | | | |
| TC(2,1,3) | 7,5 | 4 | Log-Map | 8 |
| **Turbo BCH Code (TBCH)** | | | | |
| TBCH(31,26) | 45 | 32 | Log-Map | 8 |
| TBCH(63,57) | 103 | 64 | Log-Map | 8 |
| TBCH(127,120) | 211 | 128 | Log-Map | 8 |

Table 1: Parameters of the different turbo codes used in Figure 1.

As we can see in Table 1, different BCH component codes are employed and this results in different coding rates. On the other hand, puncturing is applied to the TC code, which also results in different coding rates. We show in Table 2 the puncturing patterns employed and the resulting coding rates. The puncturing patterns seen in the table consist of two parts. Specifically, the associated different puncturing patterns represent the puncturing patterns of the parity bits emanating from the first and second decoder, respectively. Note that the puncturing patterns employed in these systems have been determined experimentally, but they are not claimed to be optimal. For procedures on designing high-rate turbo codes with the aid of puncturing the interested reader is referred to [11]. Different modulation schemes were employed, which consequently result in different effective BPS throughputs, as shown in Table 2. Prior research indicates that the bits mapped to the non-binary symbols representing the phasors of a QAM constellation exhibit different BERs [12]. These different BER subchannels are also often referred to as the different protection classes of the QAM constellation. When combining QAM with channel coding, both the parity and the original information bits can be mapped to the different protection classes. In our recent work in [3, 14] we found that the corresponding best mapping rule also depends on the error correcting power, i.e. the constraint length, of the convolutional constituent codes of the turbo codec used. For the sake of simplicity in this contribution we randomly mapped the data and parity bits to the QAM constellation points.

| Code Rate $R$ | Puncturing Pattern | Modulation Mode | BPS | Random turbo interleaver depth | Random channel interleaver depth |
|---|---|---|---|---|---|
| 0.33 | 1, 1 | BPSK | 0.33 | 228 | 684 |
| | | QPSK | 0.66 | 456 | 1368 |
| | | **Long delay** | | 34198 | 102600 |
| 0.50 | 10, 01 | BPSK | 0.50 | 342 | 684 |
| | | QPSK | 1.00 | 684 | 1368 |
| | | 16QAM | 2.00 | 1368 | 2736 |
| | | **Long delay** | | 51300 | 102600 |
| 0.75 | 100000 001000, 001000 000010 | BPSK | 0.75 | 513 | 684 |
| | | QPSK | 1.50 | 1026 | 1368 |
| | | 16QAM | 3.00 | 2052 | 2736 |
| | | 64QAM | 4.50 | 3078 | 4104 |
| | | **Long delay** | | 76950 | 102600 |
| 0.83 | 10000 00000, 00000 00001 | BPSK | 0.83 | 570 | 684 |
| | | QPSK | 1.66 | 1140 | 1368 |
| | | 16QAM | 3.32 | 2280 | 2736 |
| | | 64QAM | 4.98 | 3420 | 4104 |
| | | **Long delay** | | 85500 | 102600 |
| 0.90 | 04000 $0020_{16}$, 80000 $1000_{16}$ | BPSK | 0.90 | 615 | 684 |
| | | QPSK | 1.80 | 1230 | 1368 |
| | | 16QAM | 3.60 | 2462 | 2736 |
| | | 64QAM | 5.40 | 3694 | 4104 |
| | | **Long delay** | | 92340 | 102600 |

Table 2: Simulation parameters associated with the TC channel codec in Figure 1.

The random turbo interleaver and random channel interleaver depths are chosen such that each AQAM transmission burst can be individually decoded, i.e. burst-by-burst turbo decoding is used. Additionally, in an effort to quantify the best possible performance of the system, we also study a long-delay system, where the channel interleaver depth is chosen to be approximately $10^5$ bits in the context of all AQAM modes. The associated channel interleaver depth and the corresponding turbo interleaver depth is indicated by the 'Long delay' phrase in Table 2.

| Code Rate $R$ | Puncturing Pattern | Modulation Mode | BPS | Random turbo interleaver depth | Random channel interleaver depth |
|---|---|---|---|---|---|
| **TBCH(31,26)** | | | | | |
| 0.72 | 1,1 | BPSK | 0.72 | 494 | 684 |
| | | QPSK | 1.44 | 988 | 1368 |
| | | 16QAM | 2.88 | 1976 | 2736 |
| | | 64QAM | 4.32 | 2964 | 4104 |
| | | **Long delay** | | 74100 | 102600 |
| **TBCH(63,57)** | | | | | |
| 0.83 | 1,1 | BPSK | 0.83 | 513 | 621 |
| | | QPSK | 1.66 | 1083 | 1311 |
| | | 16QAM | 3.32 | 2223 | 2691 |
| | | 64QAM | 4.98 | 3363 | 4071 |
| | | **Long delay** | | 77976 | 94392 |
| **TBCH(127,120)** | | | | | |
| 0.90 | 1,1 | BPSK | 0.90 | 600 | 670 |
| | | QPSK | 1.80 | 1200 | 1340 |
| | | 16QAM | 3.60 | 2400 | 2680 |
| | | 64QAM | 5.40 | 3600 | 4020 |
| | | **Long delay** | | 82080 | 91656 |

Table 3: Simulation parameters associated with the TBCH channel codec in Figure 1.

Similarly to Table 2, we show in Table 3 the corresponding coding rates and the achievable BPS throughput of the TBCH codes employing various BCH component codes. Again, the turbo interleaver sizes were chosen for enabling burst-by-burst turbo decoding. Additionally, both the turbo and channel interleaver depths of the delay non-sensitive system are also shown in Table 3 again indicated as the 'Long delay' scenario.

Our studies were conducted for transmission over the COST 207 Typical Urban (TU) [15] channel. The corresponding CIR $h(t)$ is characterised as follows:

$$h(t) = 0.8507 \cdot \delta(t) + 0.3942 \cdot \delta(t - 4T) + 0.2683 \cdot \delta(t - 6T) + 0.2214 \cdot \delta(t - 7T). \quad (2)$$

Each path was faded independently according to the Rayleigh distribution and the corresponding normalised Doppler frequency was $3.27 \times 10^{-5}$. The DFE incorporated 35 forward taps and 7 feedback taps and the transmission burst structure consists a 49-symbol training sequence, which separates two 342-symbol data sequences. At each end of the transmission burst, there are 8 tail symbols. The following assumptions were stipulated. Firstly, the CIR was time-invariant for the duration of a transmission burst, but varied from burst to burst, which corresponds to assuming that the CIR is slowly varying. Secondly, perfect channel estimation and perfect knowledge of the AQAM mode used was assumed at the receiver. In practice a simple repetition code can be used for conveying the AQAM mode to the receiver. Furthermore, the modulation mode can also be detected blindly [13]. Thirdly, the pseudo-SNR at the output of the equaliser is estimated perfectly prior to transmission, which again, tacitly assumes the existence of a reliable, low-delay feedback path between the transmitter and the receiver. In practice, there will be error propagation in the DFE's feedback loop, which will degrade the performance of the system.

## 4. SIMULATION RESULTS

### 4.1. Turbo-Coded Fixed Modulation Mode Performance

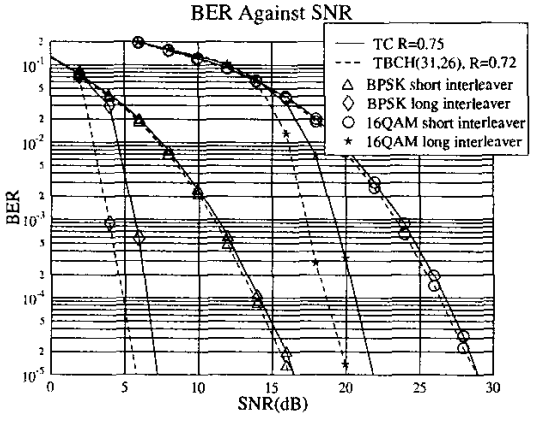


Figure 2: BER performance comparison between the rate $R = 0.75$ TC and the rate $R = 0.72$ TBCH codes using the short (burst-by-burst) and long ($10^5$ bit) channel interleaver for BPSK and 16QAM modulation schemes and transmission over the Rayleigh fading COST207 TU channel of Equation 3. The associated coding parameters are shown in Tables 1, 2 and 3.

In Figure 2 we compare, the performance of TC and TBCH codes having similar coding rates. The channel interleaver length was chosen such that it enabled burst-by-burst decoding at the receiver. Besides, we also show the best achievable performance with advent of having a long delay channel interleaver, i.e. $10^5$ bits. As we can see in Figure 2, there is virtually no performance difference between the TC and TBCH codes, when employing burst-by-burst decoding. However, if a $10^5$-bit channel interleaver is used, the TBCH codes outperform the TC codes studied by approximately $1 - 2$ dB at a BER of $10^{-4}$. Furthermore, when employing a long-delay channel interleaver, there is a huge SNR improvement of about 10 dB at BER= $10^{-4}$ as compared to the burst-by-burst decoding assisted scheme.

### 4.2. Adaptive Quadrature Amplitude Modulation Performance

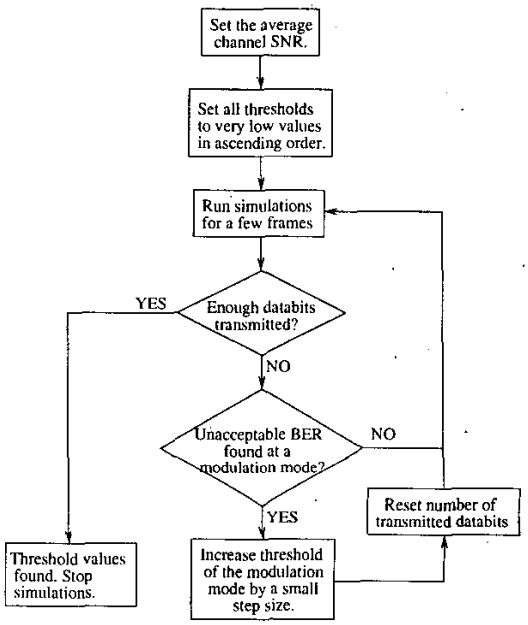


Figure 3: Procedure for determining the AQAM switching thresholds.

Let us now exploit the error correction capability of turbo codes in the context of AQAM. In our turbo coded system we propose a simple procedure for determining the AQAM switching thresholds for each average channel SNR value. In Figure 3, we show the flow chart of the simple procedure proposed for determining the AQAM switching thresholds. As we can see in the figure, we commence the procedure by setting the channel SNR, where the switching thresholds will be determined. Then we assign the lowest possible SNR switching threshold to each AQAM mode in an ascending order. At this stage, the switching thresholds are set so low that the simulated BER will be significantly higher than the targeted BER. When the simulations are started and a few frames have been received, we check whether sufficient data bits were transmitted, such that a statistically relevant BER result can be obtained. If not, the BER of each AQAM mode is checked, with the lowest-throughput modulation mode. Once an unacceptable BER was found in a particular AQAM mode, the switching

threshold of the modulation mode will be incremented by a small step size. Then, the number of transmitted data bits is reset to zero and the simulations are restarted. On the other hand, if there is no modulation mode having an unacceptable BER, more data bits will be transmitted. The entire process is repeated, until enough data bits have been transmitted, which generate a statistically pertinent average result.

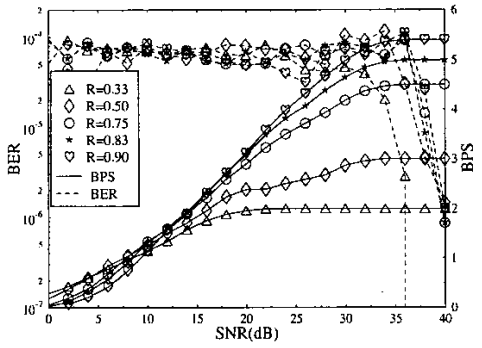


Figure 4: BER and BPS performance of burst-by-burst TC decoding using various coding rates and adaptive modulation, when communicating over the Rayleigh fading COST207 TU channel of Equation 3. The associated coding parameters are shown in Tables 1 and 2 and the target BER is $10^{-4}$.

In Figure 4 we show the BER and BPS performance of burst-by-burst TC decoding using various coding rates and adaptive modulation. The above-mentioned simple procedure was used for determining the switching thresholds. As we can see in Figure 4, the coded BER of the AQAM modem using various TC coding rates was maintained at an average of $10^{-4}$. If the same fixed switching thresholds were employed for every channel SNR, we would have an undulating coded BER curve, which would clearly deviate from the targeted BER. In Figure 4 we also plotted the BPS performance associated with each TC coding rate, which is scaled on the right hand side axis. As we can see in Figure 4, at low channel SNRs, the schemes having a lower TC coding rates will outperform those associated with the higher TC coding rates. For example, TC codes having a rate of $R \leq 0.5$ have a BPS throughput in excess of 0.5 for channel SNRs above 4 dB. However, as we increase the channel SNR, the TC coded AQAM schemes having higher coding rates outperform their lower coding rate counterparts. Furthermore, the throughput of the AQAM schemes having lower TC coding rates will saturate faster and at a lower value. For example, the TC code associated with $R = 1/3$ has a maximum BPS throughput of $6 \times 1/3 = 2$. From Figure 4 we can conclude that when the channel SNR is low, lower TC coding rates have to be employed and $R$ should be increased as the channel SNR increases.

Based on Figure 4, in our adaptive regime for every channel SNR we select the specific TC coding rate, which gives the maximum throughput in the context of the TC coded AQAM system. In Figure 5 we portray the TC coding rates selected at the various channel SNRs encountered. As we can see in the figure, the selected TC coding rate increases, as the channel SNR increases. For a channel SNR in excess of 24 dB, we can see that the TC coding rate was set to unity, which implies that the BPS throughput of the uncoded AQAM scheme becomes better, than that of

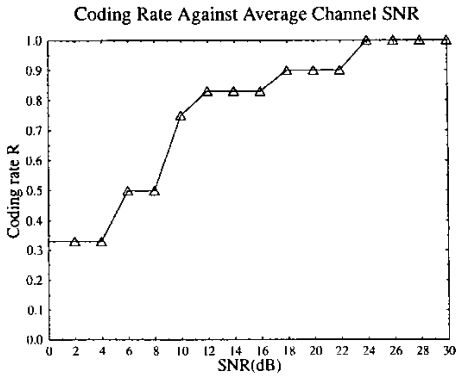


Figure 5: TC coding rates activated in conjunction with AQAM for different channel SNRs, when communicating over the Rayleigh fading COST207 TU channel of Equation 3. The associated coding parameters are shown in Tables 1 and 2 and the target BER is $10^{-4}$.

the TC coded AQAM scheme. Hence, no TC codes are activated for channel SNRs in excess of 24 dB. Previously in Figure 3, we proposed to optimise the AQAM switching thresholds individually for every channel SNR for turbo coded AQAM. Let us now extend our proposal for optimising not only the thresholds, but also the TC coding rates for every channel SNR.

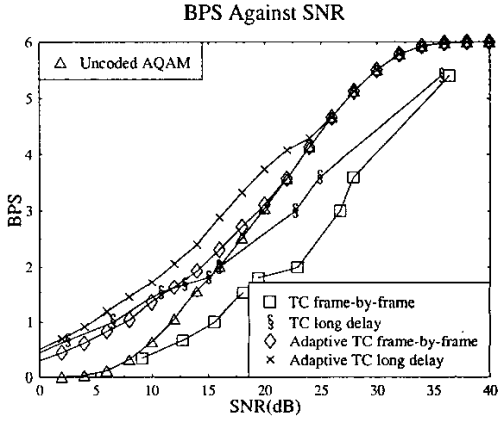


Figure 6: BPS performance comparison between uncoded AQAM, adaptive-rate TC codes using burst-by-burst decoding and long delay channel interleaver both with fixed and adaptive modulation, when communicating over the Rayleigh fading COST207 TU channel of Equation 3. The associated coding parameters are shown in Tables 1 and 2 and the target BER is $10^{-4}$.

Let us hence apply the joint switching threshold and TC coding rate optimisation techniques to the TC coded AQAM system, which we refer to this scheme in our future discourse as ORTC AQAM. In Figure 6 the curve marked with diamonds represents the BPS performance of the jointly optimised ORTC AQAM with burst-by-burst decoding. As we can see in the figure, the employment of the ORTC AQAM substantially improves the performance of the system, when the channel SNR is low. For example, at 0.5 BPS we observe a 5 dB SNR gain over the uncoded AQAM sys-

tem. However, as the channel SNR is increased, the SNR gain due to TC coding is reduced and uncoded AQAM will be employed for channel SNRs in excess of 20 dB. For channel SNRs below 13 dB we can observe in Figure 6 that the performance of the ORTC AQAM scheme is similar to that of the TC coded fixed modulation schemes using the long-delay $10^5$-bit channel interleaver. Hence, with the aid of the ORTC AQAM we can achieve as good a performance, as the long-delay optimised-rate TC coded fixed modulation scheme without incurring a long delay. More explicitly, with the aid of the AQAM system we were able to reduce the interleaving delay without compromising the BPS throughput.

On the other hand, if a long delay is tolerable in the context of the ORTC AQAM system, the $10^5$-bit channel interleaver can be employed in the system. The corresponding BPS performance is shown in Figure 6 by the curve marked with crosses. As we can see in the figure, there is a significant BPS performance improvement over the short-delay burst-by-burst ORTC AQAM system. Observe also in Figure 6 that uncoded AQAM will only be employed for channel SNRs in excess of 25 dB.

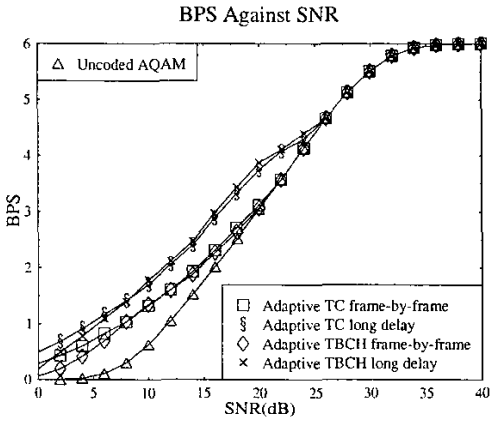


Figure 7: BPS performance comparison between uncoded AQAM, adaptive-rate TC and TBCH codes using both burst-by-burst decoding and a long-delay channel interleaver employing fixed and adaptive modulation, when communicating over the Rayleigh fading COST207 TU channel of Equation 3. The associated coding parameters are shown in Tables 1, 2 and 3 and the target BER is $10^{-4}$.

In Figures 4 and 6, we have characterised the BPS performance of the ORTC AQAM system. Let us now present the corresponding results for the ORTBCH AQAM system and compare them to the ORTC AQAM system. As we can see in Figure 7, the performance of the ORTC and ORTBCH codes is similar for the short-delay burst-by-burst turbo decoded AQAM scheme, which we have also observed in Figure 2. However for lower channel SNRs the performance of ORTBCH AQAM is inferior to that of ORTC AQAM, since in this SNR region lower coding rate TC codes were employed.

On the other hand, we also show in Figure 7 the performance of ORTC and ORTBCH AQAM using large channel interleavers. Similarly to burst-by-burst decoding, the TC codes outperform the TBCH codes for low channel SNRs. However, as the channel SNR is increased, we can see that the TBCH codes have an edge over the TC codes for channel SNRs in excess of 7 dB, although their performance gap is insignificant as compared to those observed in Figure 2. Therefore, we conclude that the employment of TBCH codes does not improve the performance of the AQAM system, although it increases the system's complexity.

## 5. CONCLUSION

In this contribution we proposed a simple procedure for determining the switching thresholds of the turbo coded adaptive modulation scheme studied. Subsequently, the achievable performance of the TC and TBCH codes were compared when using fixed and adaptive modulation schemes. It was found that the TBCH codes studied outperformed the TC coded fixed modulation schemes, when using a high-latency channel interleaver. However, both codes exhibited a similar performance, when applied in conjunction with adaptive modulation.

## 6. REFERENCES


[1] L. Hanzo, C. H. Wong and M. S. Yee, "Adaptive Wireless Transceivers", John Wiley-IEEE Press, 2002.

[2] C. Wong and L. Hanzo, "Upper-bound performance of a wideband burst-by-burst adaptive modem," *IEEE Transactions on Communications*, vol. 48, pp. 367–369, March 2000.

[3] L. Hanzo, T. H. Liew and B. L. Yeap, "Turbo Coding, Turbo Equalisation and Space-Time Coding for Transmission over Fading Channels", John Wiley-IEEE Press 2002.

[4] T. Keller, T. Liew, and L. Hanzo, "Adaptive redundant residue number system coded multicarrier modulation," *IEEE Journal on Selected Areas in Communications*, vol. 18, pp. 2292–2301, November 2000.

[5] M. Yee, T. Liew, and L. Hanzo, "Burst-by-burst adaptive turbo coded radial basis function assisted feedback equalisation," *IEEE Transactions on Communications*, vol. 49, pp. 1935–1945, November 2001.

[6] V. Lau and M. Macleod, "Variable-rate adaptive trellis coded qam for flat-fading channels," *IEEE Transactions on Communications*, vol. 49, pp. 1550–1560, September 2001.

[7] J. Torrance and L. Hanzo, "On the upper bound performance of adaptive QAM in a slow Rayleigh fading," *IEE Electronic Letters*, pp. 169–171, April 1996.

[8] B. Choi, T. Liew, and L. Hanzo, "Concatenated space-time block coded and turbo coded symbol-by-symbol adaptive OFDM and multi-carrier CDMA systems," in *Proceedings of IEEE VTC 2001 Spring*, (Rhodes, Greece), pp. 776–780, 6-9 May 2001.

[9] J. Cheung and R. Steele, "Soft-decision feedback equalizer for continuous-phase modulated signals in wide-band mobile radio channels," *IEEE Transactions on Communications*, vol. 42, pp. 1628–1638, February/March/April 1994.

[10] J. Hagenauer, E. Offer, and L. Papke, "Iterative decoding of binary block and convolutional codes," *IEEE Transactions on Information Theory*, vol. 42, pp. 429–445, March 1996.

[11] O. Acikel and W. Ryan, "Punctured turbo-codes for BPSK/QPSK channels," *IEEE Transactions on Communications*, vol. 47, pp. 1315–1323, September 1999.

[12] L. Hanzo, W. Webb, and T. Keller, *Single- and Multi-carrier Quadrature Amplitude Modulation*. Wessex, England: John Wiley & Sons, Ltd, 3rd ed., 2000. ISBN 0471492396.

[13] L. Hanzo, M. Münster, B.J. Choi and T. Keller: OFDM and MC-CDMA for Broadband Multi-user Communications, WLANs and Broadcasting, John Wiley - IEEE Press, May 2003, p 980

[14] T.H. Liew and L. Hanzo, "Space-time codes and concatenated channel codes for wireless communications," *Proceedings of the IEEE*, February 2002.

[15] Office for Official Publications of the European Communities, Luxembourg, *COST 207: Digital land mobile radio communications, final report*, 1989.